



Photoluminescence studies of Ce^{3+} activated ZnS nanophosphor

Meenakshi H¹, Rajashekhara K M², Chandrasekharreddy K³

1. Department of Physics Govt First Grade College, Chickballapur-562101, Karnataka

2. Department of Physics SJC institute of Technology, Chickballapur-562101, Karnataka

3. Department of Physics SSBN UG and PG College Anantapur- 515001, AP

Corresponding author: Email address: meena.duggu@gmail.com

Abstract: Nanoparticles of Ce^{3+} doped Zinc Sulphide have been synthesized using less concentration (0.01M and 0.03M) of dopant and Thiourea as capping agent by simple coprecipitation method at room temperature. The synthesized samples were analysed through PXRD, SEM, TEM, UV-visible and Photoluminescence studies. The size of particles calculated from XRD data are exactly matched with TEM results. The morphology of nanoparticles as observed by SEM and TEM images is almost spherical in shape. UV-visible absorption studies of prepared samples reveal that on Ce^{3+} doping band gap energy of samples slightly decreased. The different functional groups present in the samples were identified by FTIR spectra. Photoluminescence emission spectra of Ce^{3+} doped ZnS nanoparticles exhibit broad emission with peaks in visible region.

Keywords: Coprecipitation method, Thiourea, Spherical shape, Photoluminescence, Phosphor.

1. Introduction

In display application of luminescent materials mostly inorganic solids doped with rare earth impurities are used. The application of nanomaterials as light emitting display depends upon the colour output of the material. The different sulphide phosphors can be used in the field of colour conversion phosphors. ZnS is a wide gap semiconducting material, it is considered to be most famous host material because of its capability to exhibit photoluminescence at room temperature [1]. The emission properties can be studied using different dopants of rare earth elements. Luminescent materials doped with rare earth metal ions are considered as efficient phosphor material in optical devices [2]. Trivalent rare earth ions have an outer electronic configuration $5s^25p^64f^N$ where N ranges from 1(Ce ion) to 13(Yb ion), also these ions have excellent photoactive properties such as sharp emission spectra for high colour purity, broad emission bands covering the ultraviolet-visible-near infrared region and high luminescence efficiency [3,4]. These properties have attracted much attention for a wide variety of applications in the field of lighting devices like television, computer display, optical fibres, lasers [5], solid state lighting sources, optoelectronic and spintronic devices [6], photoconductivity [7] and in biomedical analysis like medical diagnosis and cell imaging [8]. The characteristic properties of the RE ions are attributable to the presence in the ion of a deep-lying 4f shell, which is not entirely filled. The electron of this shell are screened by those in the outer shells, and as a result they give rise to number of discrete energy levels. The luminescent RE^{3+} nanophosphors exhibits emission bands from visible to near infrared range depending upon host material with relatively long lifetime and high quantum yield [9]. To prepare new luminescence materials, doping of rare earth element as an activator in inorganic host material is an important key factor [10,11]. Among different rare earth ions Ce^{3+} ion is an important active ion which can show UV-visible excitation/emission due to its crystal structure dependent 4f-5d transitions [12,13]. A M Bhake and Dhoble [10], K R Bindu and E I Anila [13], N. Shanmugam et al [14], have synthesized Ce^{3+} doped ZnS nanoparticles for different applications in the field of industrial phosphor, in solid state lighting, lamp phosphor and in white LED devices. In this work Ce^{3+} doped ZnS nanophosphors are synthesized using less concentration of dopant and Thiourea as capping agent at room temperature for LED display applications. The capping agent used in the synthesis of nanomaterials controls agglomeration of particles and also improve the optical properties of materials [15,16].

2. Materials and Method

In the present study, ZnS nanophosphors without and with Cerium dopant are synthesized through chemical co-precipitation method [17,18] as follows. All the chemicals were of AR grade and were used without further purification for the preparation of nanoparticles. The chemicals used were Zinc acetate ($\text{Zn}(\text{CH}_3\text{COO})_2 \cdot 6\text{H}_2\text{O}$), Sodium sulphide($\text{Na}_2\text{S} \cdot \text{XH}_2\text{O}$) and capping agent Thiourea ($\text{CH}_4\text{N}_2\text{S}$) and Cerium(III) chloride heptahydrate($\text{CeCl}_3 \cdot 7\text{H}_2\text{O}$).

2.1 ZnS without Ce dopant: 0.2M Zinc acetate solution is prepared by dissolving 6.5847gram in 150ml (75ml of distilled water+75ml of methanol). 0.2M Na_2S solution is prepared by dissolving 3.1216 gram in 200ml (100ml distilled water+100ml methanol). 0.1M Thiourea solution is prepared by dissolving 0.761 gram of Thiourea in 100ml(50ml distilled water+50 ml methanol).0.1M Thiourea solution and 0.2M sodium sulphide solution are added separately drop by drop to 0.2M Zinc acetate solution under continuous stirring. The entire mixture is stirred using magnetic stirrer for 4 hours, then the product in the form of white precipitate is collected after centrifugation and is washed 3 to 4 times using distilled water and ethanol to remove impurities and is dried using 60 watt bulb at room temperature.

2.2 ZnS with Ce dopant[ZnS+Ce(0.01M)]: To the 0.2M Zinc acetate solution 0.01M Ce solution (prepared by dissolving 0.09314 gram of $\text{CeCl}_3 \cdot 7\text{H}_2\text{O}$ in 25ml(12.5ml distilled water +12.5ml methanol) is mixed drop by drop under stirring. Then 0.1M Thiourea and 0.2M Na_2S are added separately to the above solution drop by drop under continuous stirring .The entire mixture is stirred using magnetic stirrer for 4 hours, finally the product is collected in the form of precipitate after centrifugation and is washed 3to 4 times using distilled water and ethanol to remove impurities and is dried using 60 watt bulb at room temperature.

2.3 ZnS with Ce dopant[ZnS+Ce(0.03M)]: To the 0.2M Zinc acetate solution 0.03M Ce solution (prepared by dissolving 0.2794 gram of $\text{CeCl}_3 \cdot 7\text{H}_2\text{O}$ in 25ml(12.5ml distilled water +12.5ml methanol) is mixed drop by drop under stirring. Then 0.1M Thiourea and 0.2M Na_2S are added separately to the above solution drop by drop under continuous stirring .The entire mixture is stirred using magnetic stirrer for 4 hours, finally the product is collected in the form of precipitate after centrifugation and is washed 3to 4 times using distilled water and ethanol to remove impurities and is dried using 60 watt bulb at room temperature.

3.Instrumentation and Characterisation

The structural determination of all the samples was performed using Ultima IV X-Ray Diffractometer equipped with Ni filter for Cu $K\alpha$ radiation (0.154nm). XRD data is collected over the range 20° - 80° at room temperature. The particle size is calculated using Scherrer formula. Structural properties of samples are studied by SEM and TEM (TALOSF200SG2, 200 kV, Resolution-0.24nm) analysis. Optical properties of samples are studied using UV-Visible Spectrometer from 200 nm to 600 nm and Photoluminescence properties are studied using Spectrofluorometer (FL-1039/40) from 350 nm to 600 nm.

4.Results and discussion

4.1 XRD Studies

Results of powder X-ray Diffraction pattern of Thiourea capped, ZnS and Ce doped ZnS samples are as shown in fig 1. The three diffraction peaks corresponding to (1 1 1), (2 2 0) and (3 1 1) planes were observed for undoped and Cerium doped ZnS samples. The high intensity peak is observed at 28.98° , 28.72° and 28.52° for undoped and Ce^{3+} doped ZnS samples respectively. No extra peaks were observed due to Cerium ions and other impurities indicating that high purity of samples. Also it is observed that doping of Ce^{3+} ions did not disturb the nature of XRD graph of undoped ZnS. The size of samples was calculated using Debye Scherrer formula, $D=0.9\lambda/\beta \cos \theta$. Where D is size of particle, λ is wavelength of incident X-ray radiation (0.154nm), β is the full width at half maximum (FWHM), and θ is the diffraction angle. Also the interplanar distance 'd'and lattice constant 'a' for (1 1 1) plane of all the samples were calculated using the relations $d=\lambda/2\sin\theta$ and $a=d(h^2+k^2+l^2)^{1/2}$. (h k l) are the miller indices corresponding to the set of planes. In addition strain (ϵ) factor was also calculated using Wilson – Stokes relation $\epsilon=\beta/\tan \theta$ [16]. Calculated results of the above mentioned variables for all the samples were tabulated in the table 1.

Table 1: Structural properties of undoped and Ce^{3+} doped ZnS nanocrystallites

Sl no	Sample	Strain	Interplanar Distance (d) in nm	Lattice Constant a in nm	Size in nm
1	Undoped ZnS	0.06976	0.3075	0.53308	1.986
2	ZnS+ Ce(0.01M)	0.0685	0.3104	0.5376	2.248
3	ZnS+ Ce(0.03M)	0.0678	0.3126	0.5414	2.314

From fig 1 it is observed that 2 theta angles of high intensity diffraction peaks for Ce^{3+} doped ZnS samples were slightly shifted to lower angle side compared to the peak of undoped ZnS sample. This shifting of peaks after Cerium doping informed that Ce^{3+} ion was successfully substituted in to the ZnS host. It is found that particle size, interplanar distance and lattice constant of Ce^{3+} doped samples increases with Cerium doping concentration compared to undoped sample [14]. This might be due to the fact that ionic radius of Ce^{3+} ion is 0.103 nm and that of Zn^{2+} ion is 0.074 nm. Also it is found that Strain factor decreases with increase in size of the particles [17].

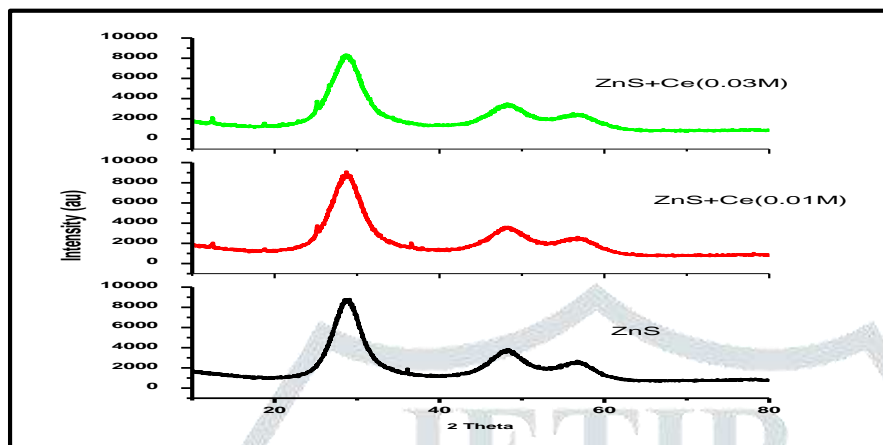


Fig 1.XRD graph of undoped ZnS and Ce^{3+} doped ZnS nanophosphors.

4.2 UV-Visible Absorption studies

Results of UV-Visible absorption spectra of undoped and Ce^{3+} doped ZnS nanophosphors are presented as shown in fig 2. The absorption peaks were observed from 260 nm to 265 nm for undoped and Ce^{3+} doped ZnS. Compared to bulk ZnS (345nm), all the samples exhibit blue shift of peaks. This is due to modification in valence band and conduction band due to quantum confinement effect. From absorption spectra it is found that peaks of Ce^{3+} doped ZnS are slightly shifted towards longer wavelength side from peak of undoped ZnS. This red shift of peaks of Ce^{3+} doped ZnS indicate that cerium might be covalently bonded with host ZnS, also strong exchange interaction might occur between the d electron of Cerium and s and p electron of the ZnS host [18]. This is also supported by slight shifting of 2 theta angle in XRD graph for Ce^{3+} doped ZnS. This red shift of peaks decreases the band gap energy value. Band gap energy values for all the synthesized samples are calculated using the relation $E=hc/\lambda$, where E is the bandgap energy of sample, h is planks constant, c is velocity of light and λ is wavelength corresponding to absorption peak of the sample[14]. The calculated values of band gap energy are found to be 4.774, 4.701 and 4.687 ev corresponding to undoped ZnS, Ce(0.01M) +ZnS and Ce(0.03M) +ZnS respectively.

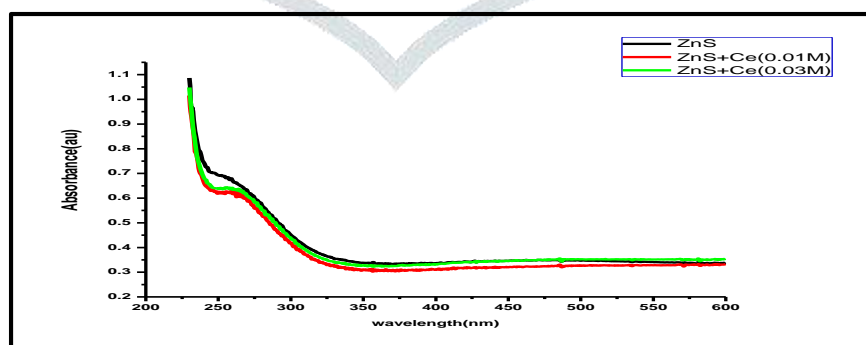


Fig 2: UV –visible absorption spectra of undoped and Ce^{3+} doped ZnS nanocrystallites.

4.3 Morphological studies

SEM studies

Scanning electronic microscopic images of ZnS and Ce³⁺-doped ZnS nanophosphors are as shown in fig 3a-c. From images it is observed that particles are almost spherical in shape for all the samples [19]. Clear morphology has been identified by TEM images.

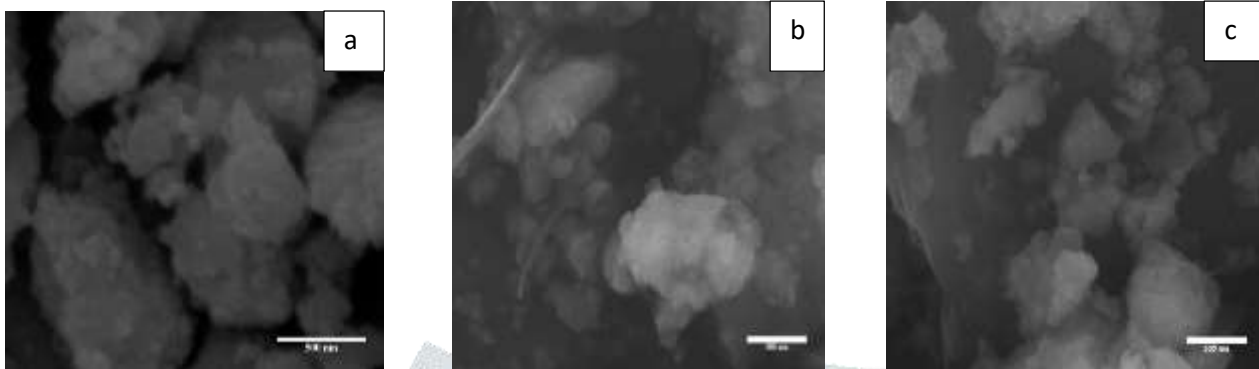


Fig 3. SEM images of (a) ZnS (b) Ce(0.01M)+ZnS and (c) Ce(0.03M)+ZnS

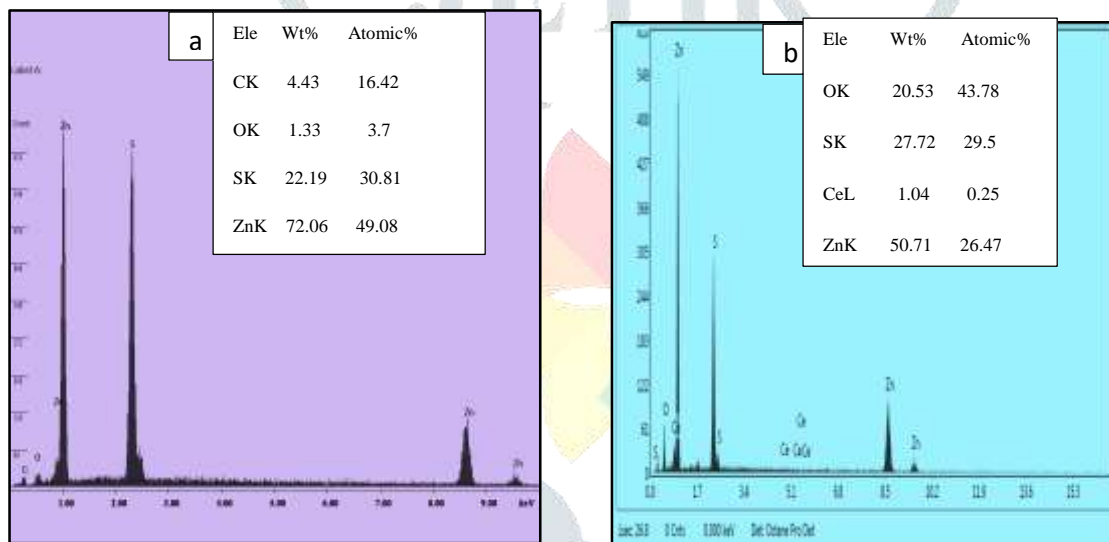


Fig 4: EDAX images of (a) ZnS and (b) (0.03M) Ce³⁺ doped ZnS samples.

EDAX images of undoped ZnS and Ce³⁺ doped ZnS nanophosphors are as shown in fig 4a-b. Substitution of Ce³⁺ ion in ZnS host is confirmed by EDAX image (b) of Ce³⁺ doped ZnS and each line in the image corresponds to individual atom. Elemental composition of each sample is mentioned in the inset of images. The advantage of taking EDAX spectrum for the sample is that, it identifies the type of X-ray [17,18].

TEM studies

TEM images SAED pattern of undoped and Ce^{3+} doped ZnS nanocrystallites are presented as shown in fig 5. TEM analysis of samples explored that, particles are in spherical shape. Also sizes measured from Tem images are well matched with XRD results. The selected area diffraction (SAED) pattern exhibits three concentric circles, informed that all samples are in nanocrystalline nature being made up of small particles. The three rings refers to (111), (220) and (311) planes of the cubic zinc blende phase of ZnS [20].

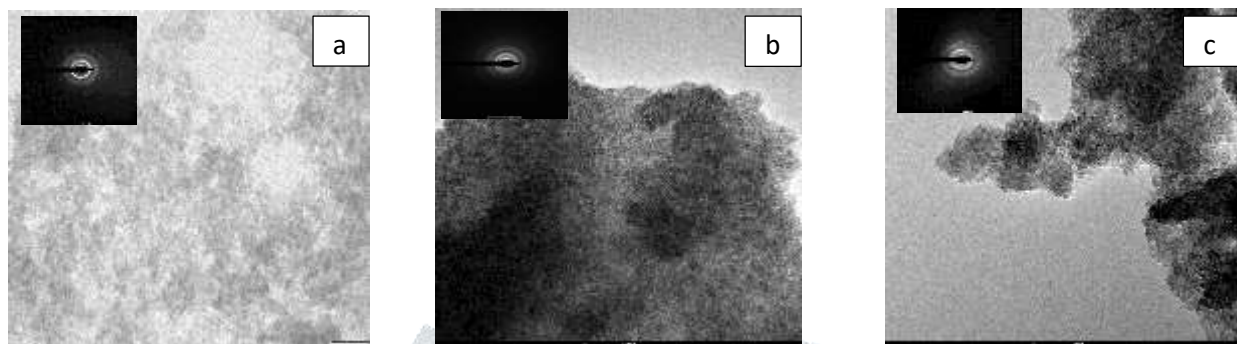


Fig 5: TEM images and SAED pattern of (a) undoped ZnS (b)Ce (0.01M)+ZnS (c) Ce(0.03M)+ZnS nanocrystallites.

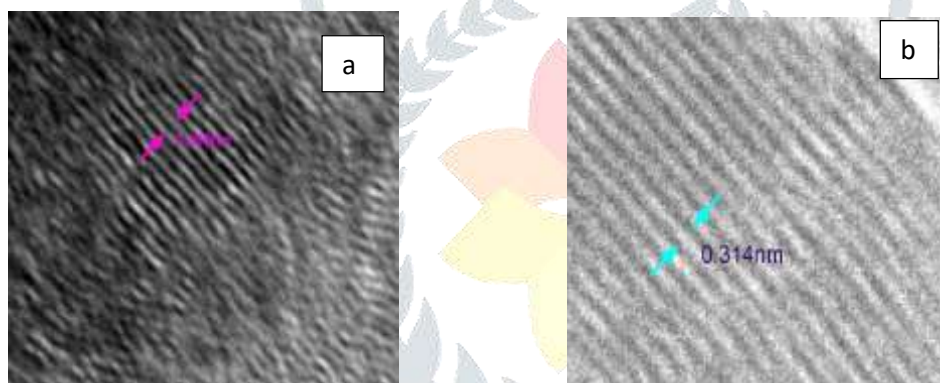


Fig 6: HRTEM images and of (a) undoped ZnS and (b) Ce^{3+} doped ZnS nanoparticles.

HRTEM images of undoped and Ce^{3+} -doped ZnS nanoparticles are depicted as shown in fig 6 a-b. It is found that the interplanar distances are in the range 0.294nm and 0.314nm respectively.

4.4 FTIR Studies

Fourier transform infrared spectra of Thiourea capped, ZnS and Ce³⁺ doped ZnS nanocrystallites are as shown in fig 7. Both the samples show a broad absorption peak at 3178.59 cm⁻¹ corresponds to O-H stretching vibration of water absorbed in the sample [14]. Peak at 1869 cm⁻¹ is observed due O-H bending of water absorbed in the sample. Peaks at 2103 cm⁻¹, 1627 cm⁻¹ are observed due to NCN stretching mode, bending mode of NH₂ conform the presence of Thiourea in the samples. Ce³⁺ doped ZnS sample show Peaks at 1551cm⁻¹ and 1395.37 cm⁻¹ due to stretching vibration of C-H group and C-O-H bending in acetate [14,18]. Peak at 1105.5cm⁻¹ in both the spectra is observed due to characteristic vibration of C-O group of acetate of nanoparticles [13]. Peak at 619.72cm⁻¹ in the spectrum of undoped sample is observed due to ZnS stretching vibration. On Ce³⁺doping however the intensity and position of the peak due to ZnS stretching vibration get slightly changed and is observed at 503.77cm⁻¹ which indicate a strong interaction might have occur between cerium and host ZnS [6,14].

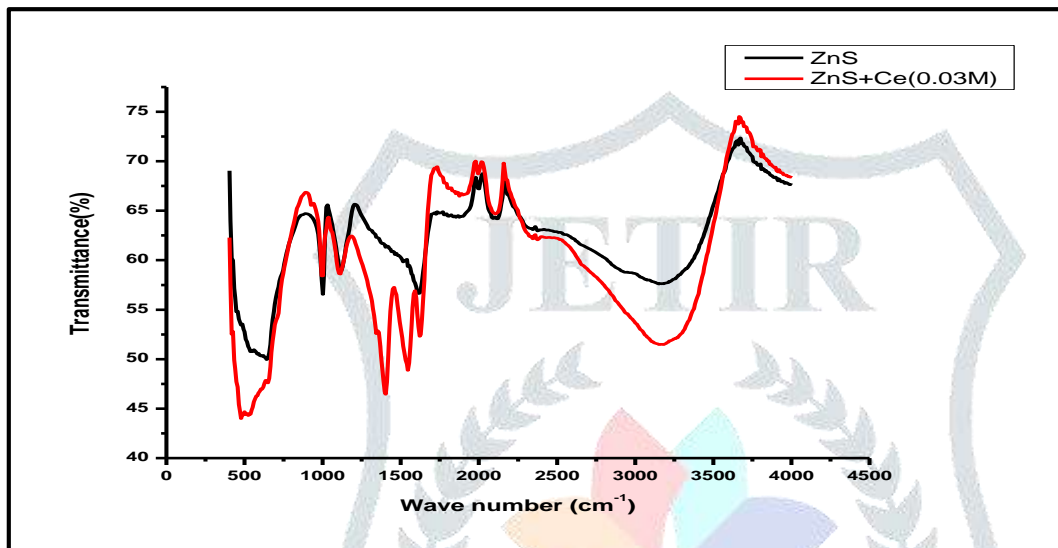


Fig 7: FTIR spectra of undoped and Ce³⁺ doped ZnS nanocrystallites

4.5 Photoluminescence studies

The Photoluminescence emission spectra of undoped ZnS and Ce³⁺ doped ZnS samples recorded using excitation wavelength 320 nm are presented as shown in fig 8. PL Studies gave information about different energy states existed between valence band and conduction band, crystal field strength, energy transfer, interaction between the luminescence centres and the host material. The broad defect emissions in ZnS may be related to the point defects which serve as luminescent sites during photoluminescence process. The point defects present in pure ZnS crystals are Sulphur vacancy, Zinc vacancy, Interstitial Zn atoms and Interstitial Sulphur atoms [16,21]. Undoped ZnS nanoparticles exhibit broad emission band with peaks at 410 and 433nm. The peak at 410nm correspond to transition from interstitial zinc to the valence band whereas peak at 435 nm was attributed to sulphur vacancy respectively [16]. Shoulder peak at 460nm is due to emission from trap states related to Zn vacancy [22]. PL emission peaks for pure ZnS nanoparticles in our report are well matched with the following reports. Neena prasad et al [16] reported the peaks at 411, 434 and 466nm respectively for pure ZnS nanoparticles. Nachimuthu Suganthi and Kuppusamy puspnanathan [22] reported the PL peaks at 408, 432 and 465nm for pure ZnS and Yt:ZnS nanoparticles.

After Cerium doping with different concentration (0.01M, 0.03M) both the samples exhibit broad emission band with peaks at 410 and 433nm respectively. This is attributed to 5d-4f transition of Ce³⁺ ions, due to doublet emission from the 5d state with lowest energy to the 2F_{5/2} and 2F_{7/2} levels of the spin orbit split of 4f ground state of Ce³⁺ ion. Shoulder peak at 460nm is also observed in Ce³⁺ doped sample due to emission from trap states [22,23]. From the emission spectra it can be seen that Ce³⁺ doping did not quench the emission peaks of undoped ZnS, but it enhanced the emission intensity. This could be due to introduction of more vacancies after Ce³⁺ doping with host material [6,13] and enhancement of radiative recombination in luminescent process [24,25].

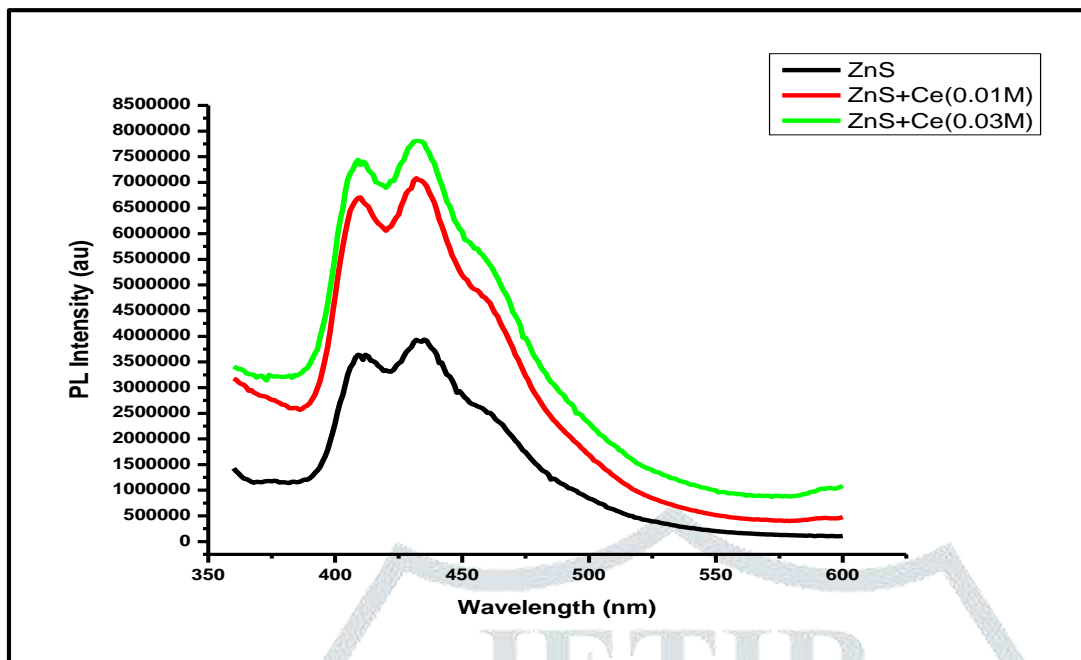


Fig 8: PL Emission spectra of undoped ZnS and Ce³⁺ doped ZnS nanoparticles.

5. Conclusion

The Rare earth Ce³⁺ ion doped ZnS and undoped ZnS nanophosphors were synthesized by coprecipitation method at room temperature using Thiourea as capping agent. All the samples were characterised under PXRD, SEM, TEM, UV-visible and PL studies. The substitution of Ce³⁺ ion in ZnS host is confirmed by PXRD and EDAX analysis. PXRD results show that shifting of peaks slightly towards lower angle side, and size of Ce³⁺ doped ZnS nanoparticles slightly increases compared to undoped ZnS nanoparticles. SEM and TEM analysis reveal that particles are almost spherical in shape and size of nanocrystallites for all the three samples calculated from TEM images are exactly matched with sizes calculated from XRD peaks. The absorption peaks of Ce³⁺ ion doped ZnS nanophosphors were shifted to higher wavelength side compared to undoped ZnS. Presence of different functional groups are clearly indicated by FTIR studies. Photoluminescence studies of pure and Ce³⁺ doped ZnS nanophosphors depicted broad emission in the visible range. After Ce³⁺ doping enhancement in emission intensity is observed. The 5d-4f transitions of Ce³⁺ in ZnS host give broad emission band. Because the 5d-4f transitions of Ce³⁺ are electric dipole allowed transition, the emission of Ce³⁺ in different hosts are very efficient. This property makes Ce³⁺ activated ZnS nanophosphors to be useful for optoelectronic devices, like lamp phosphor, industrial phosphor and in LED devices.

Acknowledgement

Authors are thankful to the Principal of SJGIT, R & D Center Chickballapur and S S B N UG and PG college Anantapur for the facilities provided in this research work, also thankful to CENSE department Bangalore for the facilities of TEM and PL studies.

Conflicts of interest

The authors declare that they have no conflicts of interest.

References:

- [1] Xiaojie Xu, Siyuan Li, Jiabin Chen, Sa Cai, Zhenghao Long, and Xiaosheng Fang, *Adv. Funct. Mater.* 2018, DOI: 10.1002/adfm.201802029.
- [2] Yuan-Chih Lin Maths Karlsson, Marco Bettinelli, *Top Curr Chem (Z)* (2016) 374:21 DOI 10.1007/s41061-016-0023-5.
- [3] Maura Cesaria, and Baldassare Di Bartolo, *Nanomaterials* 2019, 9, 1048; doi:10.3390/nano9071048.
- [4] Navadeep Shrivastava et al, *J. Mater. Chem. C*, 2017, 5, 2282—2290. DOI: 10.1039/c6tc05053k.
- [5] Harish G S, Sreedhar Reddy P, <http://dx.doi.org/10.1016/j.physb.2015.04.042>.

- [6] Nachimuthu Suganthi · Kuppusamy Pushpanathan, Journal of Inorganic and Organometallic Polymers and Materials <https://doi.org/10.1007/s10904-019-01077-4>.
- [7] Iftikhar M.Ali, Raad M.Al-Haddad, Khalid T. Al-Rasoul, Naser M. Ahmed, <http://www.ijarset.com/>, Vol. 1, Issue 4 , November 2014 , ISSN: 2350-0328.
- [8] K.V.R. Murthy, International Journal of Luminescence and Applications (ISSN: 2277-6362) Vol. 5, No. 3, August 2015. Article ID: 114. pp.302-315.
- [9] B.Yan, Springer Series in Materials Science 251, DOI 10.1007/978-981-10-2957-8_1.
- [10] A. M. Bhake, Yatish R.Parauha, S.J.Dhoble, Journal of Materials Science: Materials in Electronics <https://doi.org/10.1007/s10854-019-02559-4>.
- [11] G. Blasse et al., Luminescent Materials © Springer. Verlag Berlin Heidelberg 1994.
- [12] S. W. Joo , B. Deva Prasad Raju , G. R. Dillip , A. N. Banerjee ,J. H. Jung, Appl. Phys. A (2016) 122:102 DOI 10.1007/s00339-016-9638-1.
- [13] K.R. Bindu, E.I. Anila , <http://dx.doi.org/10.1016/j.jlumin.2017.06.047>
- [14] N. Shanmugam, S. Cholan, G. Viruthagiri, R. Gobi, N. Kannadasan, Appl Nanosci DOI 10.1007/s13204-013-0217-x.
- [15] DasariAyodhya et al.IOSR Journal of Applied Chemistry (IOSR-JAC) e-ISSN: 2278-5736.Volume 6, Issue 1 (Nov. – Dec. 2013), PP 01-09 www.iosrjournals.org .
- [16] Neena Prasad, and Balasubramanian Karthikeyan, Cite as: J. Appl. Phys. 125, 085702 (2019); <https://doi.org/10.1063/1.5083656>.
- [17] M. Gunbat , S.Horoz,O .Sahin, A.Ekinci, Digest Journal of Nanomaterials and Biostructures Vol. 13, No. 3, July - September 2018, p. 799 - 807 .
- [18] George Varughese and K. T. Usha ,Chemical science transactions. 2014, 3(4), 1354-1359,<http://www.e-journals.in> ,DOI:10.7598/cst2014.923.
- [19] M. Rajamohan Rao, S.Dastagiri , R.Jeevan kumar, (IJREAM) ISSN : 2454-9150 Vol-04, Issue-08, Nov 2018, DOI : 10.18231/2454-9150.2018.1060.
- [20] N.Shanmugam, S.Cholan, N.Kannadasan, K.SathishKumar, G.Virutagiri, <http://dx.doi.org/10.1016/j.solidstatesciences.2013.12.008>.
- [21] Xiuli Wang, Jianying Shi, Zhaochi Feng, Mingrun Li and Can Li , Phys. Chem. Chem. Phys .,2011,13,4715–4723,DOI: 10.1039/c0cp01620.
- [22] Nachimuthu Suganti and Kuppusamy Pushpanathan, Surface Review and Letters, Vol. 25, No. 6 (2018) 1850063 , World Scientific Publishing Company DOI:10.1142/S0218625X18500634.
- [23] Sudheesh K. Shukla, Eric S. Agorku, Hemant Mittal, Ajay K. Mishra*, Chemical Papers 68 (2) 217–222 (2014) DOI: 10.2478/s11696-013-0442-5
- [24] K.Manojkumar et al, Journal of Superconductivity and Novel Magnetism <https://doi.org/10.1007/s10948-018-4972-5>.
- [25] Huaming yang, Chenghuan Huang, Xiaohui Su, Aidong Tang, Journal of Alloys and compounds 402 (2005) 274-271, doi:10.1016/j.jallcom.2005.04.150.

